

9. SITE 298

The Shipboard Scientific Party¹

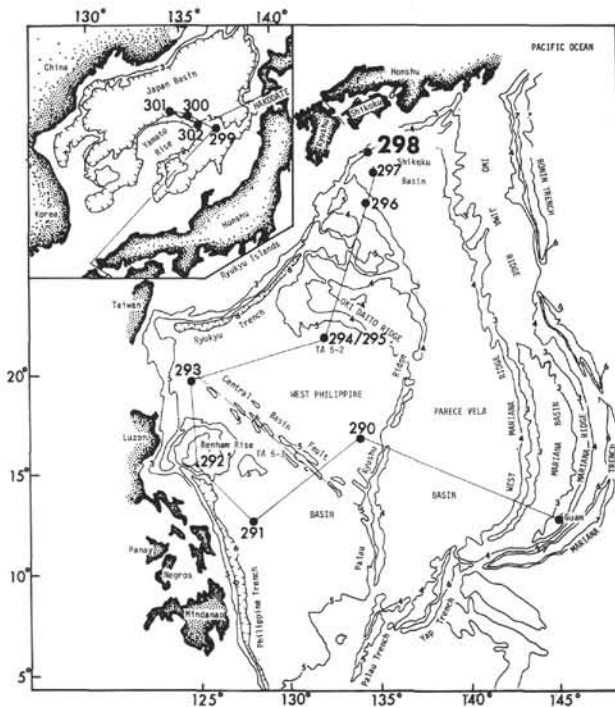


Figure 1. Location map and Glomar Challenger Leg 31 track for region around Site 298. From map: "Topography of North Pacific," T. E. Chase, H. W. Menard, and J. Mammerickx, Institute Marine Resources, Geol. Data Center, Scripps Institution of Oceanography, 1971. Contour depths in kilometers; scale 1:6,500,000.

SITE DATA

Position: 31°42.93'N; 113°36.22'E

Water Depth (from sea level): 4628 corrected meters (echo sounding)

¹James C. Ingle, Jr., Stanford University, Stanford, California; Daniel E. Karig, Cornell University, Ithaca, New York; Arnold H. Bouma, Texas A&M University, College Station, Texas; C. Howard Ellis, Marathon Oil Company, Littleton, Colorado; Neville S. Haile, University of Malaya, Kuala Lumpur, Malaysia; Itaru Koizumi, Osaka University, Osaka, Japan; Ian MacGregor, University of California at Davis, Davis, California; J. Casey Moore, University of California at Santa Cruz, Santa Cruz, California; Hiroshi Ujiié, National Science Museum of Tokyo, Tokyo, Japan; Teruhiko Watanabe, University of Tokyo, Tokyo, Japan; Stan M. White, California State University at Fresno, Fresno, California; Masashi Yasui, Japan Meteorological College, Tokyo, Japan; Hsin Yi Ling, University of Washington, Seattle, Washington.

Bottom Felt At: 4659 meters (drill pipe)

Penetration:

Hole 298: 611 meters
Hole 298A: 98 meters

Number of Holes: 2

Number of Cores:

Hole 298: 16
Hole 298A: 1

Total Length of Cored Section:

Hole 298: 145.5 meters
Hole 298A: 9.5 meters

Total Core Recovered:

Hole 298: 66.8 meters
Hole 298A: 0.4 meters

Percentage of Core Recovery:

Hole 298: 45.8%
Hole 298A: 4.2%

Oldest Sediment Cored:

Depth below sea floor: 611 meters
Nature: Silt/shale
Age: Early Pleistocene

Principal Results: Drilled on the lower, inner slope of Nankai Trough off Shikoku Island, Japan, Hole 298 encountered a stratigraphic section consisting of 183 meters of Holocene(?) - late Pleistocene turbidite cobble-size fragment bearing clayey and silty sand and silty clay underlain by 427 meters of late to early Pleistocene clay(stone), silt (stone), and clayey-silty sand. Anomalous compaction and small-scale structures become evident below a depth of 300 meters and increase in intensity downward. Below 500 meters, the beds are overturned, with dips averaging 13°. Structures in Hole 298, together with reflection profiles, demonstrate the accretion of an overturned fold consisting of tectonically dewatered trench sediments as a result of subduction at a rate of 3 cm/yr.

BACKGROUND AND OBJECTIVES

Background

One of the major gaps in our knowledge of marine tectonics concerns the kinematics and mechanics of processes which are assumed to take place in trenches. Although there is a great deal of circumstantial evidence to indicate that oceanic lithosphere is subducted and that some crustal components are accreted at or near trenches, there is little direct information about the process responsible and the structures which develop. Investigations have been greatly impeded by technical limitations in the great water depths and by the lack of coherent acoustic returns from within the critical rocks of the inner slope.

Among the problems presently being discussed are the origin of the turbidites in the deformed mass attributed

TABLE 1
Coring Summary, Site 298

Core	Cored Interval Below Bottom (m)	Cored (m)	Recovered		Remarks ^a
			(m)	(%)	
Hole 298					
1	0.0-3.0	3.0	0.2	7.0	Punch Core
Wash	3.0-126.5				
2	126.5-136.0	9.5	3.5	37.0	
Wash	136.0-174.0				
3	174.0-183.5	9.5	0.6	6.0	
4	183.5-193.0	9.5	3.8	40.0	
5	193.0-202.5	9.5	2.1	22.0	
Wash	202.5-278.5				50 bbls mud
6	278.5-288.0	9.5	3.0	33.0	
Wash	288.0-297.5				
7	297.5-307.0	9.5	3.0	33.0	
Wash	307.0-316.5				Increase in drilling rate
8	316.5-326.0	9.5	1.8	19.0	
Wash	326.0-335.5				
9	335.5-345.0	9.5	2.9	31.0	Slower drilling rate through Core 16
Wash	345.0-364.0				
10	364.0-373.5	9.5	5.7	60.0	50 bbls mud
Wash	373.5-392.5				
11	392.5-402.0	9.5	4.8	51.0	
Wash	402.0-421.0				
12	421.0-430.5	9.5	6.4	67.0	
Wash	430.5-468.5				
13	468.5-478.0	9.5	7.3	77.0	
Wash	478.0-516.0				50 bbls mud
14	516.0-525.5	9.5	5.0	53.0	
Wash	525.5-563.5				50 bbls mud
15	563.5-573.0	9.5	9.5	100.	
Wash	573.0-601.5				
16	601.5-611.0	9.5	7.2	76.0	
Total	611.0	145.5	66.8	46.0	
Hole 298A					
Wash	0.0-50.5				
1	50.5-60.0	9.5	0.4	4.0	Heat flow taken at 60 meters
Wash	60.0-98.0				Heat flow taken at 98 meters
Total	98.0	9.5	0.4	4.0	

^aFigure 3 contains graphs of drilling rates and lithology.

heat-flow measurement was taken at 60 meters. This same sediment was washed from 60 to 98 meters where an additional heat-flow measurement was attempted (Table 1).

Tropical depression Ellen recurved south-southwest and reached Site 298 at about 0100, 23 July with winds of 45-60 mph, and seas of 8-12 feet. This required premature retrieval of the heat probe and abandonment of Hole 298A. A major power failure occurred while bringing the heat-flow instrument out of the hole. The loss of computer and automatic positioning resulted in drift of the ship 762 meters (2500 ft) from the hole. The drill string and heat probe were pulled from the hole. Ultimately, inspection revealed that the bit and two drill collars had broken off during drifting of the ship, with damage to three bumper subs and two other drill collars. Site 298 was departed under storm conditions at 1300, 23 July.

LITHOLOGY

Drilling operations at Site 298 reached 611 meters below the sea floor recovering 17 cores. The two holes (298, 298A) represent the deepest penetration into a

trench inner wall and provide a good example of the lithology and structural geology of sedimentary deposits incorporated into this environment. For consideration of lithology and structural geology, the cores from both holes are grouped together and subdivided into two lithologic units (Table 2 and Figures 3 and 4).

Unit 1

Unit 1 makes up Core 1 through Core 5, Section 1, 120 cm in Hole 298 and Core 1 in Hole 298A (0-194.2 m). This unit is composed predominantly of clayey silt, and clayey and silty-sand, with minor amounts of small cobbles of silty claystone, calcareous sandstone, and limestone.

The included Pleistocene cobbles serve to distinguish Unit 1 from Unit 2. The cobbles occur as irregularly shaped clasts up to 10 cm long. The clasts occur in both muds and sands. Macroscopic and microscopic inspection of sand beds indicates the presence of up to 25% granule and sand-size lithic fragments of similar composition. The larger cobbles show weathering rinds and borings.

TABLE 2
Unit Descriptions, Depths, Thicknesses, and Ages, Site 298

Unit and Descriptions	Depth (m)	Thickness (m)	Age
1 Cobble-bearing clayey and silty sand, and silty-clay	0-94.20	194.20	Late Pleistocene-Holocene (?)
2 Fissile clay (stone), silt (stone), and clayey and silty sand	94.20-611	427.25	Early Pleistocene

The sand of Unit 1 is medium to fine grained, and occurs in beds up to 1 meter thick. One bed is graded, although this may be a drilling artifact. The foraminifera present were apparently reworked from the neritic environment, probably by turbidity currents.

Unit 2

Unit 2 is found in Core 5 (excepting the top 120 cm) through Core 16, Hole 298 (194.2-611 m). The dominant lithologies are fissile clayey silt (stone), silty clay (stone), silt (stone), and clayey and silty sands. Below Core 8, Section 1 the cores were not split in order to preserve their structural integrity. Clayey silt (stone) and silty clay (stone) are the most abundant lithologies of Unit 2. In addition to clay, quartz, and feldspar, these deposits include a few percent volcanic ash and nannofossils, with traces of radiolarians, sponge spicules, and diatoms. The muddy sediments become consolidated below Core 5. In general, the muds of Unit 2 are over-consolidated (see Physical Properties section). Conversely, the sand beds remain unconsolidated/unlithified throughout Unit 2.

Sand and silt beds occur in 8 out of 12 cores of Unit 2. These beds range up to 16 cm thick with a maximum grain size of medium sand. They are both graded and ungraded; the graded beds are characterized by sharp bases and indistinct tops. Positive identification of silt-clay graded beds in Cores 8-16 required close examination of locally split core surfaces. The grading, sharp bases and indistinct tops, and poor sorting of the sands and silts of Unit 2 suggest deposition by turbidity currents.

Ash deposits occur in Cores 5, 9, and 10. One bed is 9 cm thick and distinctly graded. The primary constituents of the ash beds are volcanic glass and feldspar.

Lithologic Interpretations

Both Units 1 and 2 are composed of an interbedded sequence of hemipelagic muds and turbidity current deposits. Significant concentrations of nannofossils, but only traces of foraminifera in the hemipelagic muds, indicate deposition above the local carbonate compensation depth probably near the lysocline. The ubiquity of density current deposits suggests ponding of Units 1 and 2 in a basinal environment, probably the Shikoku Trench. A minor part of Unit 1 may have accumulated in synformal depressions of the trench inner wall during uplift; however, neither the seismic reflection profile nor PDR record show any ponded sediment.

The conspicuous sand beds and cobbles of Unit 1 suggest it is more proximal than Unit 2 which contains predominantly mud rocks with minor sand and silts. This upward coarsening (Unit 2-1) (Figure 4) could be a time-dependent variation associated with Pleistocene climatic fluctuations (of which there were several). Since the lower Pleistocene rocks at this site did not show a similar variation, this single coarsening episode is probably not climatically induced. The upward coarsening could also be due to a migrating submarine distributary channel. However, if the Shikoku Trench is supplied from the north (Hilde et al., 1969), any distributary channel would tend to remain relatively stationary along the inner wall due to Coriolis force and/or landward tilting of the trench fill during subduction. Finally, the coarser sediments of Unit 1 could also be due to a seaward transgressive proximal facies. This relationship implies accretion of the trench inner wall and/or subduction of the trench sediment prism.

Unit 1 turbidites are of neritic derivation (see section on Biostratigraphy) and could have picked up some of the rock clasts during movement to the deep sea floor. However, some of the clasts are included in the hemipelagic muds suggesting local derivation probably from the structural scarp of the trench inner wall. Thus, the mud beds which include mudstone clasts are probably gravity slide deposits (olistrostromes) derived from the trench inner wall.

STRUCTURAL GEOLOGY

The main structural feature of Site 298 is long wavelength folding which cannot be analyzed within an individual contiguous core. Therefore, most structural study was directed towards the recording of orientations of bedding, hackly fracture surfaces (possible cleavage) with the intent of building a statistical picture of deformation (Tables 3-5, Figure 5).

Structural Elements

Bedding is the primary structural datum by which the fold is defined. A secondary S-surface cross-cutting bedding occurs in Cores 8 through 16. Superficially this structure is manifested by discontinuous hairline fractures (<1 cm long) inclined at low angles (10°-20°) to bedding. Where recognized, the separation of secondary fractures ranges from 1 mm to about 5 mm. Macroscopic and microscopic observations did not detect any obvious mineral orientation associated with these fractures. These hackly fractures are interpreted as

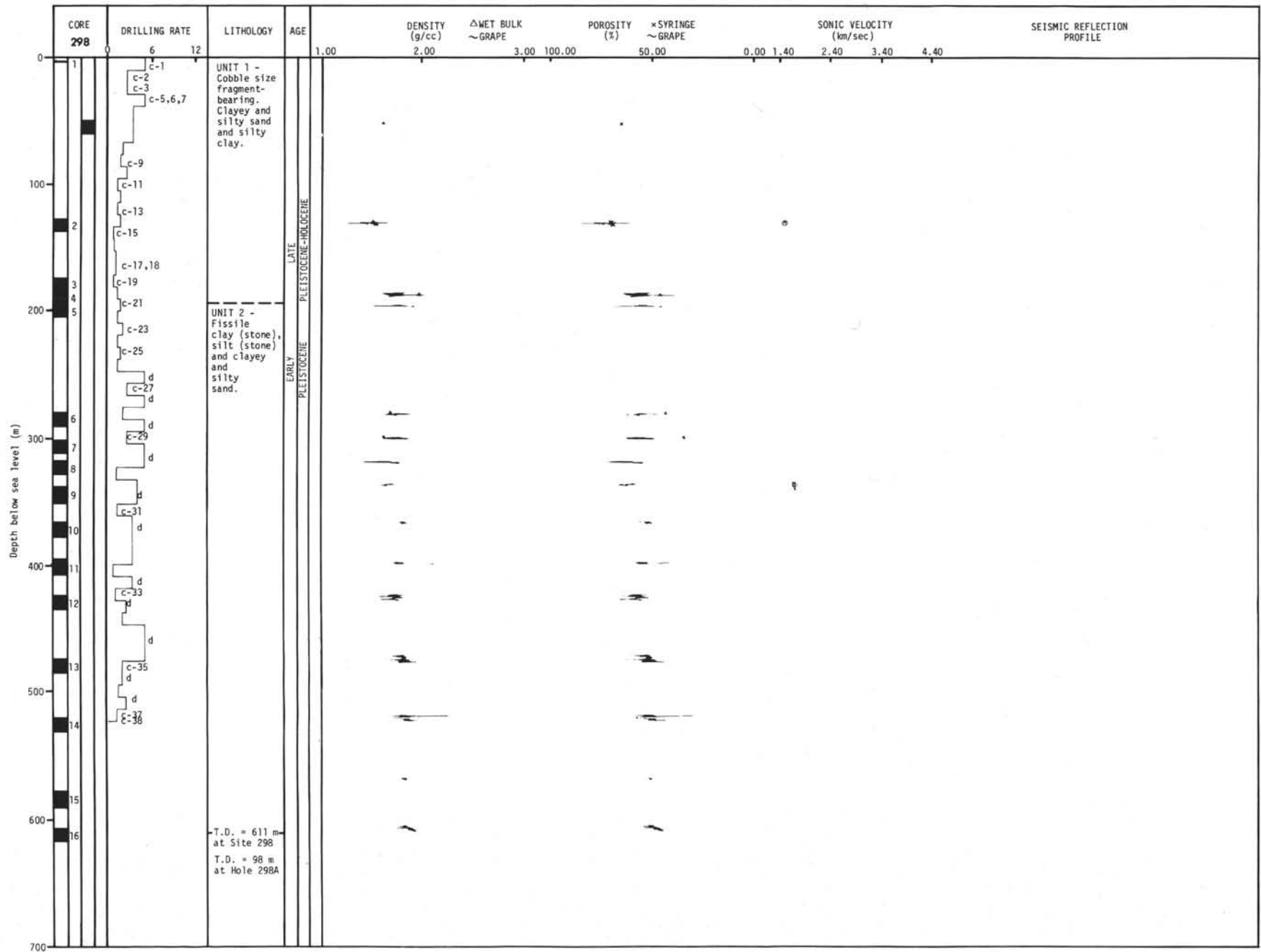


Figure 3. Hole summary diagram, Site 298.

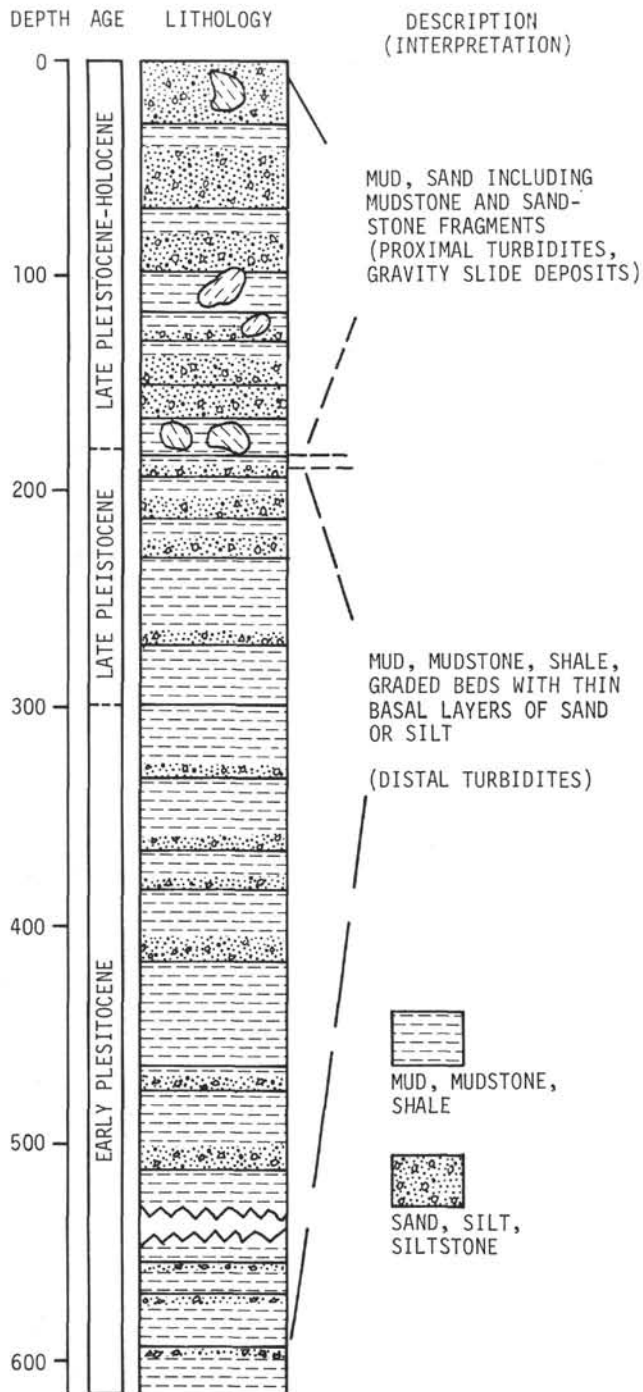


Figure 4. Generalized stratigraphic sequence, Site 298.

an incipient cleavage. Support for this interpretation is found in the symmetry of orientation of the fractures to the fold axial plane, nevertheless their origin needs to be more firmly documented.

High angle fractures (average 51°) occur in the consolidated rocks at the site. These surfaces are regular planes locally occurring in conjugate sets and/or showing slickensides. According to Howard Ellis (personal communication, 1973) slickensided surfaces commonly occur in drill cores of clay shale. They apparently

develop in response to drilling stresses which exceed the confined shear strength of the shale. The extent, planarity, and high-angle orientation of these drilling-induced surfaces generally allow them to be distinguished from the natural cleavage fractures. These high-angle fractures grade into artificially produced kink bands.

Orientation Analysis

The cores from Site 298 have no horizontal orientation. It is assumed that they were cored vertically since the maximum deviation of drill holes at this depth averages less than 2° . The apparent intersections of bedding and cleavage are horizontal suggesting a similar orientation for the major fold axes. Since the cores are locally broken, it is assumed that the beds on both flanks of any large-scale fold dip in the same direction. The large-scale symmetry of folding can be analyzed, but horizontal orientations cannot be predicted. However, the site survey revealed horizontal co-linear ridges paralleling the trench axis which allow the inference of the folding trend.

The limiting factors in defining the geometry of the fold are: (1) the direction of tops and altitude of bedding, (2) the orientation of the axial surface, and (3) the external geomorphic surface of the fold. By definition axial surface contains the hinge lines of all folded layers. For a symmetrical fold this surface bisects the interlimb angle and splits the fold into mirror images. The plane symmetrical to the bedding of Cores 13 and 14 (upright) and 15 and 16 (overturned) is inclined at about 9° and provides one approximation to the axial surface. However, if the fold is asymmetrical due to tectonic thinning of the lower limb, the axial surface would be steeper than 9° . An observed cleavage is probably of the axial plane variety (see below). If so, the average inclination of cleavage provides another approximation of the axial surface. The plane of symmetry to cleavage in Cores 13 and 14 versus Cores 15 and 16 is inclined at 12.8° . The profiles presented by Hilde et al. (1969) indicate landward dipping faults and a possible seaward asymmetry of folds. Thus, a combination of seismic reflection and core orientation data indicates that the axial surface of the cored anticline dips from 9° to 13° toward the trench inner wall.

Sedimentary layering apparently follows the form of the external surface of the ridge along the lowest portion of the trench inner wall (Hilde et al., 1969). The bathymetry (ignoring any hyperbolic distortion) of the basin and ridge at Site 298 was used as a constraint on the form of the folded surface. Modifications are included for minor infilling of the basin at the site and for slumping off the seaward face of the ridge.

Based on the preceding data and assumptions, two possible geometries are presented for the cored anticline. One (Figure 5B) is based on an axial surface dipping at 9° (from symmetry of bedding) and another (Figure 5A) utilizes an axial surface dipping at 12.8° (from symmetry of cleavage). The resulting fold would be classified as tight in both cases and as either recumbent (first case) or overturned (second case). Although the cleavage orientations are less numerous and accurate than those of bedding, the real fold is probably more like that por-

TABLE 3
Inclination of Bedding Planes, Cleavage, and Drilling Induced Fractures

Average Depth of Core	Sample	Inclination/Bedding		Inclination/Cleavage		Inclination of Drilling Fractures	Bedding Tops	
		Section Average	Core Average	Section Average	Core Average			
322	8-1	0	3	—	20	65	↑	
	8-2	5						
340	9-1	0	2	28	28			
	9-2	3		27				
369	10-1	5	10	16	22	40		
	10-2	8		29				
	10-3	13		22				
	10-4	15		—				
397	11-1	14	8	—	—		Upright	
	11-2	9						
	11-3	6						
	11-4	2						
426	12-1	9	7	12	17	45		
	12-2	9		22		50		
	12-3	3		18		60		
	12-4	5		—		68		
473	12-5	8	7	—	24	35		
	13-1	0		—				
	13-2	8		17		45		
	13-3	14		—		45		
521	13-4	6	2	30	17		Boundary	
	14-1	6		19				
	14-2	0		10				45
	14-3	0		22				
606	14-4	0	12	35	0		Overturned	
	15-1	22		10				
	15-2	14		—				
	15-3	8		13				10
	15-4	11		—				
	15-6	13		—				90
	16-1	13		0				
	16-2	13		0				
16-3	11	—						
	16-4	9	—					
	16-5	14	—					

Note: Data averaged for each section and core. Dashes (—) indicate intervals for which no cleavage measurements were recorded.

TABLE 4
Average Inclinations of Bedding and Cleavage on Upright and Overturned Limbs of the Anticline

	Average Dip of Bedding	Average Dip of Cleavage
Upright Beds		
1. Core 8 through 14	5.6	21.3
2. Cores 13 and 14	4.5	20.5
Overturned Beds		
3. Cores 15 and 16	13.5	5.0

Note: In (1) the average begins at Core 8 since here we noted the first evidence of broad deformation defining the overturned anticline; (2) compiles structural data for an upright section approximately equal in thickness and adjacent to the overturned section (3).

trayed in Figure 5A since the overall geometry is likely to be asymmetrical.

If the upper limb of the fold is entirely composed of trench turbidites, then the half wavelength of the overturned anticline is approximately 500 meters. This

dimension is within the range of half wavelengths measured from subaerially exposed trench deposits (Moore, 1973). The frequency of coring precludes any major dip reversals in the upper limb; however, parasitic folds may occur.

Stratigraphic evidence nowhere demands major thrust faults, but small-scale thrusts might be present throughout the cored sequence. Thrust faults could form by the attenuation of the lower limbs of overturned anticlines. If so, the dip of the thrust planes would be subparallel to the axial surface of folding.

Structural Interpretations

The sequence cored at Site 298 consists of trench deposits which have suffered overturned-recumbent tight folding early in their structural history. The fold axes apparently trend parallel to the trench axis and the fold axial surface is probably overturned seaward. The deformed rocks show an apparent incipient cleavage which developed during subduction.

The folded rocks of Site 298 are overconsolidated for their present depth of burial indicating that they have been strain hardened by excess stress of tectonic origin.

TABLE 5
Axial Surfaces and Planes of Cleavage Symmetry
Determined From Average Dips of Bedding and
Cleavage on Limbs of Overturned Anticline

Portions of Fold Limbs Compared		Inclination of Plane Symmetrical to Bedding (Axial Surface)	Inclination of Plane Symmetrical to Cleavage
Upright	Overtured		
Core 8 through 14	Cores 15 and 16	9.6	13.2
Cores 13 and 14	Cores 15 and 16	9.0	12.8

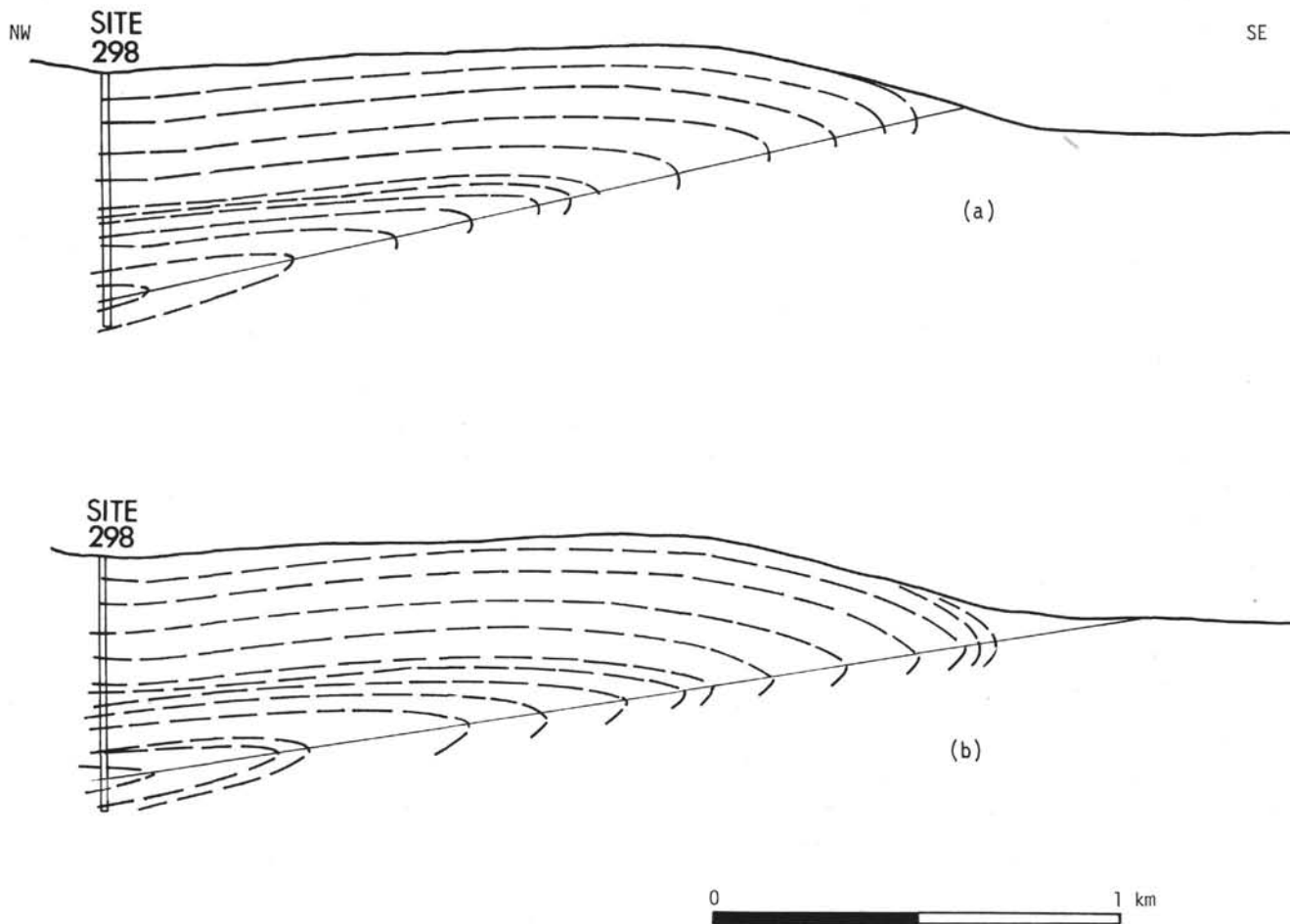


Figure 5. *Fold reconstructions. Inclination of axial surface in (a) defined by plane symmetrical to cleavage surfaces of Cores 13-16. Inclination of axial surface in (b) determined from plane symmetrical to bedding in Cores 13-16. (a) is preferred reconstruction (see text for explanation).*

The lithologic and structural data from Site 298 prove that subduction of trench sediments does not necessarily form a mélangé nor possibly even a broken formation.

PHYSICAL PROPERTIES

The abnormal fissile character of the silt-rich claystones places most of the physical property data outside a comparison range with the other sediments encountered on Leg 31.

Bulk Density, Porosity, and Water Content

Since the sediment from Cores 5 through 16 consists of a fissile clayey mudstone that normally was broken into pieces within the core liner, the GRAPE analog records are very erratic (Figure 3). Estimating the average over part or total of a curve could easily result in errors. For that reason many section curves had to be divided into portions.

When the record from a section was divided into a top and a bottom part, the density value obtained from the top part was always lower than that of the bottom part. The reason for this has to be due to the fissility of the material, which will create more hair cracks the longer the material has to move up into the core barrel. In this case the rocks endure more friction over a longer period of time as well as vibration.

Also, when comparing the water contents, obtained via the syringe method or the cube or chunk method for the same interval, it becomes apparent that the chunk method gives higher values. The main reason for this discrepancy is due to the fissile nature of the sediment which breaks up when the syringe is inserted. This not only results in inaccuracies in volume, but allows water vapor to escape instantly when the sample is extruded in the small metal weighing dish.

Both groups of density values (GRAPE and laboratory) clearly reveal that values of 1.5-1.55 g/cc are normal for the upper sediment above Core 3. The fissile sediments (Cores 5 through 16) reveal some scattering, but nevertheless show that only a minor downward increase in density exists over the 437-meter interval cored. Since the values are higher than normally encountered in clayey sediments at equivalent burial depths, this points to pressure influences other than overburden or removal of former overburden. It also suggests that the pressure did not vary much for the total package of cored fissile sediments.

Only one piece from Core 10, Section 4 was measured on the GRAPE unit outside its liner. If core diameters are assumed to be 2.65 inches the analog record indicates a bulk density of 1.83 g/cc and a porosity of 53.8%. Using the actual diameter of 2.45 inches, the density increases to 1.98 g/cc, and the porosity then becomes 43.9%. While it is not valid to assume that all densities should be increased by 0.15 g/cc due to minor diameter variations, a general increase by 0.1-0.15 g/cc seems proper. This increase places all laboratory values consistently lower than the GRAPE values as had been the case with the findings from other holes during Leg 31.

The water-content values are opposite from the bulk densities, and due to less scattering (Figure 3), they make the above-mentioned conclusions more positive.

Vane Shear

Vane-shear measurements on the upper cores from Holes 298 and 298A are too few to allow comparison with similar measurements carried out on other holes. The material has a very high water content, and consequently a low shear strength. Drilling deformation is the main reason for these low strength values.

Unit 2 (Cores 5 through 16), consisting of fissile silt-rich claystones, did not lend itself too well to vane-shear measurements. Normally cracks appeared when inserting the vane, while in other cores the material was too hard. The limited number of data from Cores 2 through 6 may for that reason not be reliable also due to the wide scattering of values.

The wide variety of data obtained on Sample 6, CC, while still in its steel container, proves that

measurements in the horizontal plane have little or no value in this material that breaks up into little flakes under little pressure.

Sonic Velocity

The fissile nature of the sediment made it impossible to obtain more than a few data (Table 6, Figure 3) in spite of the many attempts made. Two measurements on Core 2 resulted in a sonic velocity of 1.52 km/sec. Cores 4 through 8, as well as Cores 10 through 16, had a very high attenuation due to their fissile nature. Two measurements on Core 9 resulted in an average sonic velocity of 1.73 km/sec, which probably is lower than the actual in situ velocity.

Thermal Conductivity

Thermal-conductivity measurements were made on the cored sediments obtained from Hole 298 and in situ temperature measurements were measured at subbottom depths of 60 and 90 meters in Hole 298A. The results of these measurements are shown on Table 7 and summarized on Figure 6.

Thermal-conductivity values seem to show a twofold breakdown: values averaging 2.0×10^{-3} cal/cm sec $^{\circ}$ C characterize a sandy sediment, while a slightly higher mean value of 2.6×10^{-3} cal/cm sec $^{\circ}$ C characterizes a dry clay. It is possible that in situ thermal conductivities of the dry clay (shales) would be higher than the measured values, because of the lower water content of these sediments under higher pressures.

Heat Flow

The in situ temperatures measured at 60 meters in Hole 298A were steady and seemed to be reliable values. Data from the 98-meter depth could not be reduced because of computer problems. The 60-meter reading showed an initial steady temperature value much lower than the value recorded for the sediment. This value is assumed to represent bottom-water temperatures (Figure 7).

Between the temperatures recorded for the bottom water and the sediment, the thermal gradient was estimated to be 0.67×10^{-3} $^{\circ}$ C/cm. Unfortunately, no thermal-conductivity measurement was made for the upper 60 meters. The only available conductivity data from the former surface observation are 2.25×10^{-3} cal/cm sec $^{\circ}$ C at 31 $^{\circ}$ 45'N, 133 $^{\circ}$ 46'E and 2.19×10^{-3} cal/cm sec $^{\circ}$ C at 31 $^{\circ}$ 47'N, 134 $^{\circ}$ 08'E. Assuming 2.2×10^{-3} cal/cm sec $^{\circ}$ C for the thermal conductivity, the heat-flow value is 1.5×10^{-6} cal/cm 2 sec.

TABLE 6
Sonic-Velocity Measurements, Site 298

Sample (Interval in cm)	Depth in Hole (m)	Velocity (km/sec)
2-3, 40.0	129.90	1.523
9-1, 44.0	335.94	1.709
9-4, 44.0	340.44	1.729

TABLE 7
Thermal Conductivities Measured at Site 298

Sample (Interval in cm)	Hole Depth (m)	Thermal conductivity in 10^{-3} cal/cm sec °C		
		Needle Probe	Average	From Water Content
2-3, 20	130	2.00	2.00	2.09 ± 0.11
4-2, 60	186	2.19	2.39	2.67 ± 0.17
4-2, 100	186	2.59		
5-2, 35	195	2.49	2.58	
5-2, 110	196	2.67		3.22 ± 0.22
7-2, 14	299	2.31	2.39	
7-2, 85	300	2.47		
9-1, 30	336	2.22	2.33	
9-1, 85	336	2.43		
9-1, 144-150	336			3.02 ± 0.20
10-2, 60	366	2.71	2.71	
11-4, 55	398	2.61	2.53	
11-4, 120	398	2.59		
12-3, 40	424	2.40		
12-3, 90	425	2.33	2.47	
12-4, 40	426	2.55		
12-4, 100	427	2.54		
13-3, 40	472	2.67	2.64	3.20 ± 0.26
13-3, 110	473	2.61		

Thermal Conductivity in 10^{-3} cal/cm sec °C

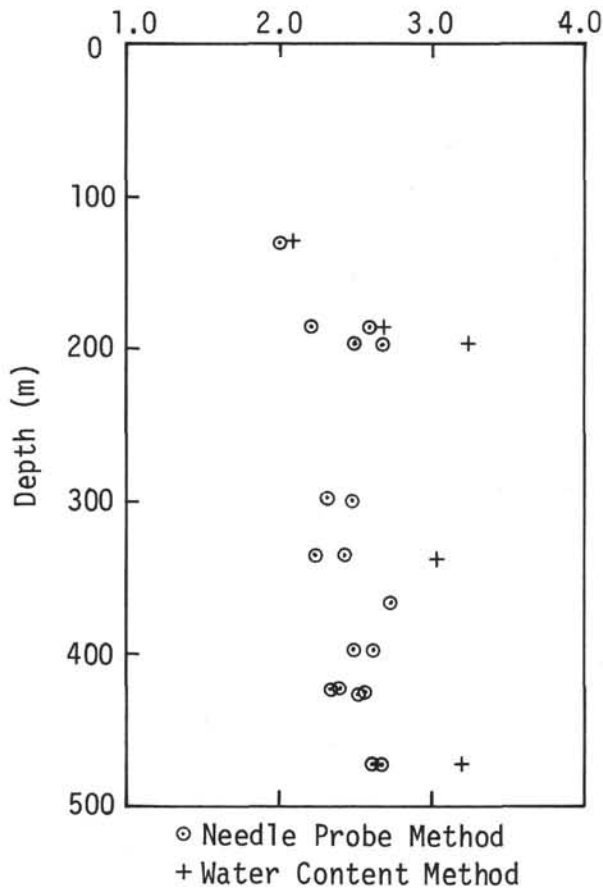


Figure 6. Thermal-conductivity results, Site 298.

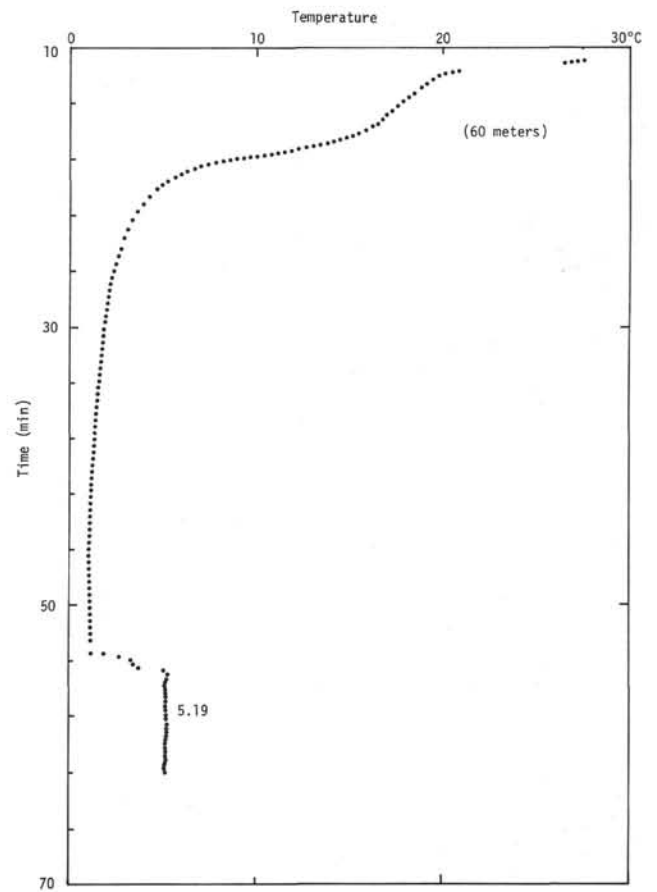


Figure 7. Heat-flow results, Site 298.

GEOCHEMICAL MEASUREMENTS

Alkalinity, pH, and salinity measurements are summarized in Table 8.

Alkalinity

The average alkalinity of the 10 samples is 11.06 meq/kg. The 10 values and the average are all above the surface seawater reference value of 2.54. The highest value (21.70) is found in Core 4, Section 2 186.5 meters below the sea floor. A rather sharp increase in values occurs between Cores 2 and 4 (3.62 to 21.70, respectively). The two cores represent two different lithologic units. A sharp drop in values occurs between Cores 11 and 13 (13.10 to 8.80). Both cores are in Unit 2.

pH

The average of the pH values obtained by punch-in and flow-through methods were all below that of the seawater reference (8.27 and 8.14). Four punch-in pH values averaged 7.88, while 10 flow-through values averaged 8.02. The punch-in pH values show a tendency to decrease with depth, while flow-through show two zones of decreasing values and two zones of increasing values, relative to the average of 8.02.

Salinity

Ten salinity measurements in Hole 298 averaged 34.4‰. The average value is the same as the overlying seawater value of 34.4‰. The trend of the salinity values shows two zones of relatively low values (Cores 4 to 7 and 11, 13, and 14), with high values occurring in Cores 9, 15, and 16. This is similar to the trends shown for pH.

PALEONTOLOGIC SUMMARY

Introduction

Nannofossils, foraminifera, radiolarians, diatoms, and a few scattered silicoflagellates were recovered from most of the samples in Holes 298 and 298A, with all groups indicating a Holocene (?) and Pleistocene age for the entire section.

Cores 1 through 4 in Hole 298 (0-193 m) and Core 1 along with a heat-flow probe sample in Hole 298A (0-183 m) contain few to abundant well-preserved specimens of all fossil groups with all species pointing to a late Pleistocene or Holocene age for this interval. The base of the calcareous nannofossil *Emiliani huxleyi* Zone which approximates the Holocene/Pleistocene boundary² occurs in Core 4, Section 1 (146.5 m). The remainder of Core 4 through the top of Core 7 (146.5-318.0 m) in Hole 298 is late Pleistocene in age by nannofossil zonation.

Cores 7 through 16 (318-611.0 m) contain nannofossils, planktonic foraminifera, and diatoms with calcareous nannofossils indicating an early Pleistocene age for these sediments.

Calcareous Nannofossils

Samples from Core 1 through Core 4, Section 1 of Hole 298 and Core 1 of Hole 298A contain a moderately to well-preserved nannofossil assemblage with commonly occurring specimens of *Emiliana huxleyi*, which clearly places these samples in the Holocene-late Pleistocene *E. huxleyi* Zone.

The absence of *E. huxleyi*, and the presence of *Gephyrocapsa oceanica* in Sample 4, CC through Core 7, Section 1 permits placing samples from this interval in the late Pleistocene *G. oceanica* Zone. The remainder of the samples from this hole (Samples 7, CC through 16, CC) contain commonly occurring specimens of *G. caribbeanica*, but *G. oceanica* is no longer present, which suggests that this sample interval belongs in the early Pleistocene *G. caribbeanica* Subzone.

Foraminifera

Occurrence of foraminifera is generally restricted to the sandy lithofacies which is developed mainly in the upper layers of Cores 1 through 4. The fauna consists of

²The base of this zone is equivalent to an age of 0.2 m.y.B.P. according to Bukry (1973).

TABLE 8
Summary of Shipboard Geochemical Data, Site 298

Sample (Interval in cm)	Depth Below Sea Floor (m)	pH		Alkalinity (meq/kg)	Salinity (‰)	Lithologic Unit
		Punch-in	Flow through			
Surface seawater reference		8.25	8.14	2.54	34.4	
2-3, 135-150	130.9	7.95	8.19	3.62	34.6	Unit 1
4-2, 144-150	186.5	7.94	7.91	21.70	34.1	
6-1, 144-150	280.0	7.83	7.91	16.03	34.4	
7-1, 144-150	299.0	7.82	8.03	13.59	34.1	
9-1, 144-150	337.0	—	8.11	15.54	35.2	
11-3, 144-150	397.0	—	7.92	13.10	33.8	Unit 2
13-4, 144-150	474.5	—	7.88	8.80	34.1	
14-3, 144-150	519.0	—	8.02	6.35	34.1	
15-3, 144-150	568.0	—	8.15	5.57	34.6	
16-2, 144-150	605.0	—	8.08	6.35	34.9	
Average		7.88	8.02	11.06	34.4	

probable late Pleistocene planktonic species accompanied by benthonic species characteristic of subtropical to temperate, neritic environments (including *Pseudorotalia gaimardii*, *Ammonia takanabensis*, etc.).

Among 11 core-catcher samples from the lower muddy facies of Hole 298, only Core 12 yields Pleistocene juvenile forms reflecting the minor sand content within the facies. An exclusively planktonic foraminiferal fauna is present in an ash layer within the muddy facies in Sample 9-1, 70-73 cm.

Radiolarians and Silicoflagellates

Radiolarians and silicoflagellates at Site 298 are disappointingly low in abundance. Rare to few specimens of a moderate to well-preserved Quaternary species were recovered in Hole 298, Cores 1 and 2 and Hole 298A, Core 1. This assemblage consists of radiolarian taxa which are commonly found in the surface sediments of a warm-water region. All the remaining samples (Cores 3 through 16) of Hole 298 and sediments collected from the heat-flow probe at 98 meters of Hole 298A contain either rare undiagnostic species or are completely barren of these microfossils.

Only a few silicoflagellates were recovered in samples from Cores 1, 8, and 12 of Hole 298, and in a heat-flow probe sample of Hole 298A (98 m).

Diatoms

Diatoms occur throughout the samples at Site 298 except for Cores 9, 11, 15, and 16, where they are very few or completely absent. Species present include: *Actinocyclus ehrenbergi*, *Cocconeis scutellum*, *Diploneis bombus*, *D. smithii*, *D. suborbicularis*, and *Grammatophora oceanica*, and fresh-water species: *Cocconeis placentula* v. *euglypta*, *Cymbella* spp., *Epithemia zebra*, *E. sorex*, *Gomphonema* spp., and *Melosira granulata*.

Cores 1, 2, 12, and 13 of Hole 298, and a sample from the heat-flow probe at 98 meters of Hole 298A belong to the *Pseudoeunotia doliolus* Zone (Holocene-Pleistocene), as determined by the presence of the nominated taxon.

SUMMARY AND INTERPRETATIONS

Summary

Hole 298 penetrated 611 meters into the lower inner slope of the Nankai Trough and demonstrated that marked compaction and deformation associated with subduction occur very close to the interface between undeformed trench wedge sediment and the acoustically opaque material of the trench slope. Almost the entire drilled section comprises a turbidite sequence which was deposited in the trench wedge. The sequence consists of clay, silt, and a smaller amount of sand all of Quaternary age.

The upper 200 meters or so include semilithified cobbles, which are used to define a separate upper stratigraphic unit. These cobbles seem most likely to have come down the inner slope, perhaps in canyons which dissect the deformed sediments. They were probably transported in pieces about the size recovered.

Because of low recovery and drilling deformation, there is little information from the upper 100 or 150

meters of the hole. However, the ages and sedimentation rates indicate that little of any material has been removed from the top of the section, and that sedimentation has been nearly continuous. A change from trench floor to slope sediments somewhere in the upper 150 meters is expected and might be placed near 125 meters, where a sharp drop in penetration rate and sample porosity occur (Figure 3).

The main sedimentary sequence becomes irregularly finer grained with depth and includes very few sand beds in the lowermost 100 meters, where the sediment approaches a fissile silty claystone or shale. This downward progression of lithology apparently reflects both an increase in deformation and a gradual facies change as the drill penetrated loci of deposition changing from the inner edge of the turbidite wedge toward the outer edge.

Deformation must begin almost from the surface because of the anomalously difficult drilling conditions and because there are no coherent acoustic returns on either the seismic reflection or PDR profiles. However, there are no megascopically observable deformation characteristics in the sediment. Visible cleavage begins near 300 meters and becomes more pronounced with depth. Near the bottom of the hole, there is a definite fissility in the rocks. Although there may be local intervals in which the bedding dips steeply, by far the majority of dips are less than 10°. The average dip above 525 meters is 6°, but in the bottom two cores (about 550 to 611 m), the strata are overturned and have dips averaging 13.5°. Cleavage in the upright beds has an average dip of 23° and in the overturned section it has a dip of 4°, in the same direction as bedding. The geometry of overturned fold with a horizontal B axis is thus indicated. Trends of fold axes cannot be determined from the core data, but the high degree of parallelism among the ridges which comprise the lower trench slope (Figure 2), implies that these represent folds and that B axes are colinear with the trench axis.

Interpretation

The Nankai Trough is a unique trench because it is less than 5000 meters deep, and yet the large number of high-magnitude shallow focus earthquakes (Kanimori, 1972) and rapid uplift of the southern Japanese coast (Fitch and Scholz, 1971) suggest that subduction is presently at rates in the range of 3-8 cm/yr. No anomalous results from investigations of this trench were expected because its shallow depths are thought to reflect the geometry of the preexisting continental margin and the relatively shallow oceanic crust being subducted (Karig and Sharman, in press). The results of Hole 298, integrated with those of Hole 297, the site survey, and the available seismic reflection profiles (Figure 8) (Hilde et al., 1969; Karig and Sharman, in press) permit the construction of an internally consistent geometric and kinematic model. This model may be valid for at least those trenches consuming plates which are heavily laden with sediment and slowly subducting.

The sediment cover entering the Nankai Trough includes two units; the general cover of the Shikoku Basin and a wedge of turbidites deposited along the trench ax-

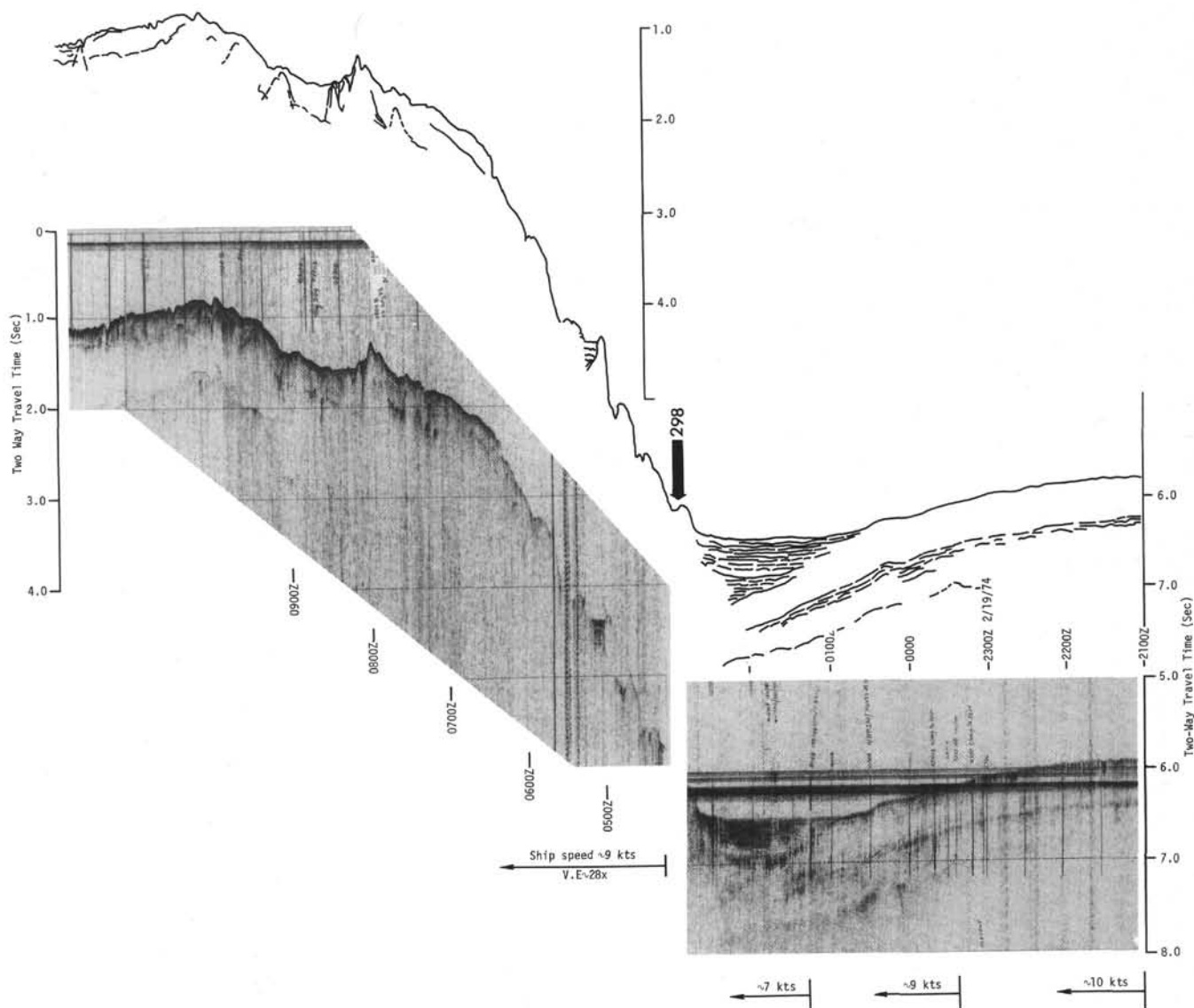


Figure 8. Glomar Challenger seismic reflection profile across the Nankai Trough and Shikoku slope, together with interpreted profile.

is. The 800-meter-thick basin section, sampled at Site 297, is composed of 330 meters of hemipelagic muds overlying a more turbidite-rich section. As this section is traced toward the trench on reflection profiles, the only change that can be discerned is a thickening of the uppermost hemipelagic unit immediately adjacent to the trench wedge. This increase in depositional rate might best be ascribed to density of nepheloid-type currents associated with turbidite deposition on the flat-floored trench wedge.

The trench wedge of the Nankai Trough in the vicinity of Site 298 is approximately 17 km wide and 700 meters thick at the base of the inner slope where deformation disrupts the acoustic picture. In a manner similar to that described in the Aleutian Trench (Kulm et al., 1973), the uppermost part of the underlying basin sediments thin beneath the wedge in the direction of the inner trench slope. This thinning, which represents a

trenchward decreasing interval of deposition, can be used to determine the rate of sedimentation in the trench wedge. However, a lack of reflectors in the uppermost hemipelagic basin sediments beneath the Nankai Trough makes this determination more difficult.

On both the *Seifu Maru* (unpublished) and *Glomar Challenger* reflection profiles, which run along similar tracks, the thinning of the pelagics beneath the turbidite wedge at the edge of step totals 0.15 sec. If it is assumed that a normal increase in acoustic velocity and moderate compaction with depth takes place through the sediments involved, a difference in thickness of 110 to 125 meters is obtained. The sedimentation rate in the late Pleistocene section at 297 is near 100 m/m.y., but because the trenchward increase in the thickness of the hemipelagics is attributed to deposition very close to the wedge, a comparative rate near 150 m/m.y. is more likely correct.

The 0.69-sec acoustic travel time through the trench floor sediments is assumed to represent an uncompacted thickness of between 675 and 700 meters. The 0.8 m.y. it took to lay down the 110-125 meters of pelagics equivalent to the wedge sediments thus define an average sedimentation rate in the trench wedge of between 0.85 and 0.9 km/m.y. The one other well-determined sedimentation rate determined for a trench wedge is the 2 km/m.y. value of Kulm et al. (1973) in the eastern Aleutian trench. This doubled rate is expected because of the glacially enhanced erosion of a much larger and more rugged drainage area feeding the Aleutian trench.

Sedimentation rates can be related to subduction rates through an analysis of the trench wedge as a two-dimensional sediment reservoir. The instantaneous amount of sediment fed to this reservoir is the sedimentation rate (D) times the width of the trench wedge (W). That leaving is the subduction rate (S) times the thickness of the wedge corrected for compaction at the inner edge of the trench slope (T). If the wedge remains the same size, then the two factors can be equated ($D \times W = S \times T$); otherwise the results must be discussed as an inequality. The amount of material entering the Nankai Trough is about 15 km²/m.y. per unit length of arc. If a stable wedge is assumed, the subduction rate would be 2.2 cm/yr, or far less than has been postulated on the basis of seismological and geodetic data. If the geophysically determined rate of 3-8 cm/yr is accepted, then the trench wedge must be rapidly shrinking.

There is no evidence that the sedimentation rate in the trench axis has increased sufficiently to permit a sufficiently rapid recent increase in subduction rate. The relatively tight zonation in the Quaternary sediments drilled in Hole 298 permit calculation of reliable sedimentation rates after the effects of compaction and tectonic thickening are recognized.

The porosity drop in Hole 298 (Figure 3), from nearly 70% to less than 40% at the fold axis, undoubtedly represents sample bias toward the clay-rich section, but few sand beds occur in the most severely compacted deeper section. The compaction adjusted rates are less than those calculated for the present trench wedge, and decrease downward reflecting the more distal turbidite facies. Because no Pliocene strata were penetrated in the core of the fold, a simple, compaction-corrected sedimentation rate from 300 meters to 550 meters in the hole must exceed 500 m/m.y. However, the fine-grained nature of the sediment, and less rapid deposition of the overlying coarser sediments, would suggest rates significantly less than 400 m/m.y. This evidence for tectonic thickening reinforces the indications for thickening seen in the lower turbidites of the trench wedge on reflection profiles (Figures 8 and 9).

Thus, in the section of the trench wedge sampled by Hole 298, the average sedimentation rate was about 500 m/m.y. (Figure 10), and under steady-state conditions, with no change in dip of the downgoing plate beneath the wedge, the subduction rate should have been near 1.3 cm/yr. This lower rate, for a slightly earlier time period, is consistent with the initiation of trough conditions about 3 m.y. ago, as indicated by the results of Hole 297. Moreover, slow subduction without a

morphologic trough may have been taking place since the middle Miocene in a manner similar to that now taking place along the Washington and Oregon coasts (Silver, 1972). In the Fuji Valley, which marks the landward extension of the Nankai Trough, and presumably the plate boundary, severe folding of middle Miocene and younger age rocks has been recognized (Matsuda, 1962; Kimura, 1966).

Although these figures are estimates, they generate an internally consistent picture of a subduction zone that has been increasing in rate of consumption since mid or late Miocene. It is difficult to see how the present rate could exceed 3 cm/yr, which in turn suggests that the Philippine-Asia pole of rotation now lies not far to the northeast of the east end of the Nankai Trough.

Horizontal displacement of the sediments in the drilled fold, during the 0.2 to 0.3 m.y. it took to develop, should be in the range of 2 to 4 km, assuming that roughly $\frac{3}{4}$ of the displacement related to subduction occurs beneath the lowermost trench slope. From these estimates, it can be seen that there is little necessity for a major thrust fault between the drilled fold and the presently developing step area. Deformation can, for the greater part, be accommodated by folding and by shear-induced thickening.

The fold does not involve the hemipelagic sediments underlying the turbidite wedge, which supports the idea that the wedge turbidites are sheared off the deeper pelagic section and accreted at shallow depths (Karig, 1974). This decollement may break into the inverted limb of the lowest fold and surface at the base of the trench slope (Figure 9).

On most profiles across the western Nankai Trough, a zone of warped and slightly uplifted wedge turbidites lies in front of the first major ridge constituting the inner slope (Figure 9). This zone is particularly well observed on Figure 3 of Hilde et al. (1969), where there is a suggestion that not only basement but also the lower turbidite-rich sequence of the Shikoku Basin section lies undeformed beneath. Reflection or diffraction patterns indicate that axial surfaces and faults in the wedge turbidites dip landward. On the *Glomar Challenger* record (Figure 8) there is stratigraphic continuity at the top of the wedge turbidites and rapid thickening of the lower wedge area which must be structural in origin. The easiest and most logical structural interpretation is that the shallow folds are the surface expression of a set of developing thrusts, or a zone of shears reaching upward from the decollement surface near the base of the wedge turbidites (Figure 9). With time, this area will develop into another fold ridge such as was drilled at Site 298.

A progression of structures can be envisaged where the upper, more rigid wedge sediments are first warped and buckled in front of the major active shear surface. A new decollement then begins to develop beneath this surface and finally replaces it, adding one more packet of folded sediments to the inner trench slope. Decollement occurs near the base of the turbidite wedge because the immediately underlying hemipelagic strata are much weaker and have significantly higher water contents than do the trench turbidites (Karig and Sharman, in press). In addition to affording a zone of weakness, this level probably develops very high pore pressures, further

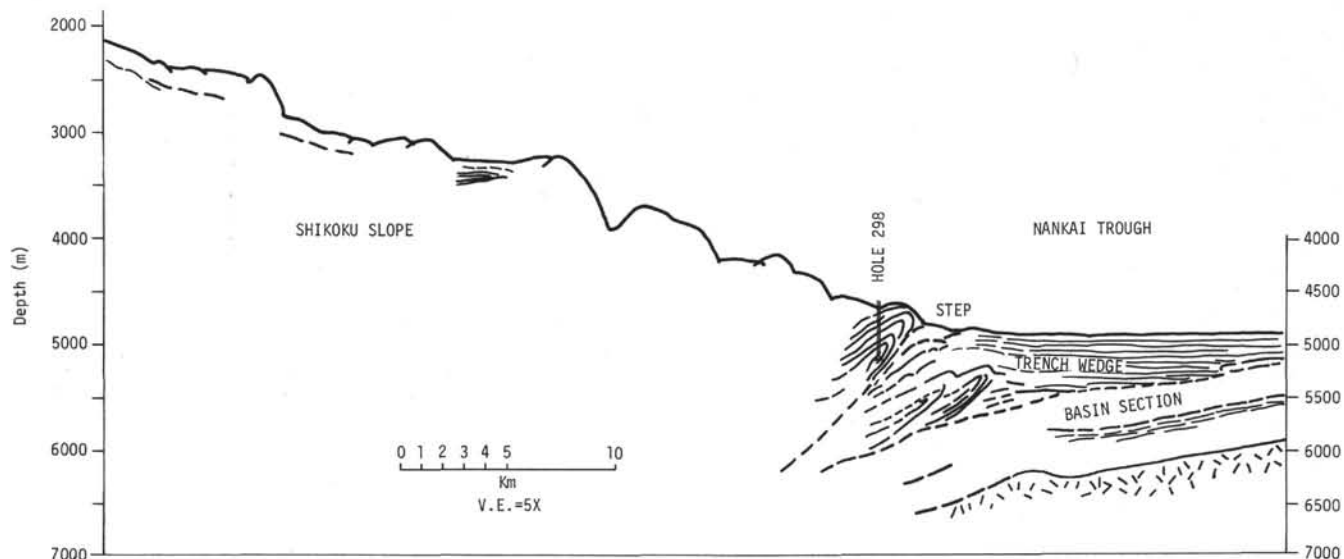


Figure 9. Interpretive geologic section across the Nankai Trough, based on Hole 298 and reflection profiles of *Glomar Challenger* and others (Hilde et al., 1969).

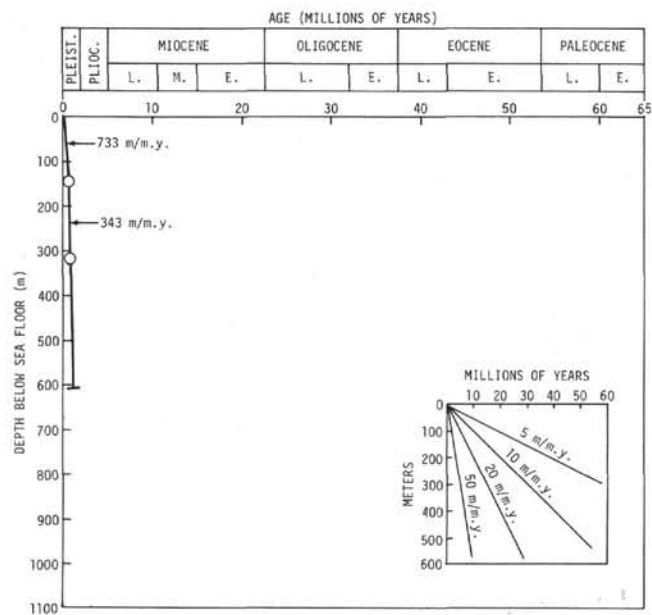


Figure 10. Estimated rate of sedimentation for Site 298 based on calcareous nannofossil zonation (Ellis, this volume) and the time scale of Berggren (1972). Note that the curve does not include a correction for compaction.

reducing its resistance to shear. It is then not difficult to see why the sediments of the turbidite wedge, even if they represent only a minor fraction of the total thickness of strata fed to the subduction zone, constitute the great bulk of the deformed pile which later becomes exposed.

Progressive accretion of ridges consisting of wedge turbidites along the base of the trench slope accounts for the sets of linear ridges seen in the site survey (Figure 2).

Between the lowermost ridges little or no sediment has collected, but the fill steadily increases upward, undoubtedly representing hemipelagic and lesser amounts of slumped deposits moving down the slope. Sediments in these linear ponds appear to be tilted in both directions. The lowermost definable pond on the *Glomar Challenger* profile dips seaward, and the next pond up the slope has a seaward dipping surface, but the dip reverses with depth. We feel that these ponds measure large-scale tilting of structures within the slope from the 10° dip acquired during the initial deformation toward a steeper landward dip (Moore, 1973) rather than representing rotated slump masses (von Huene, 1972). A tectonic origin better explains the upward thickening of slope sediments and enlarging ponds than does gravity gliding. It also appears that the inner trench slope becomes reorganized into larger steps from the base upward, with greater relief between the highs and lows (Figures 3, 4). This transition might be accomplished by the localization of shear into fewer, more discrete zones coupled with uplift and rearward tilting, and would support the idea that deformation continues, at a steadily decreasing rate, from the trench axis to the trench slope break (Karig, 1974).

REFERENCES

- Berggren, W., 1972. A Cenozoic time-scale—some implications for regional geology and paleobiogeography: *Lethaia*, v. 5, p. 195-215.
- Bukry, D., 1973. Coccolith stratigraphy, eastern equatorial Pacific, Leg 16, Deep Sea Drilling Project. In van Andel, T. H., Heath, G. R., et al., Initial Reports of the Deep Sea Drilling Project, Volume 16: Washington (U.S. Government Printing Office), p. 653-712.
- Creager, J. S., Scholl, D. W., et al., 1973. Initial Reports of the Deep Sea Drilling Project, Volume 19: Washington (U.S. Government Printing Office).

- Fitch, T. J. and Scholz, C. H., 1971. Mechanism of underthrusting in southwest Japan: a model of convergent plate interactions: *J. Geophys. Res.*, v. 76, p. 7260-7292.
- Hilde, T. W. C., Wageman, J. M., and Hammond, W. T., 1969. The structure of Tosa Terrace and Nankai Trough off southeastern Japan: *Deep-Sea Res.*, v. 16, p. 67-75.
- Kanimori, H., 1972. Tectonic implications of the 1944 Tonankai and 1946 Nankardo earthquakes: *Phys. Earth Planet. Interiors*, v. 5, p. 129-139.
- Karig, D. E., 1974. Evolution of the Western Pacific: *Ann. Rev. Earth Planet. Sci.*, v. 2, p. 51-76.
- Karig, D. E. and Sharman, G., in press. Accretion and subduction in trenches: *Geol. Soc. Am. Bull.*
- Kimura, T., 1966. Tectonic movements in the southern Fossa Magna, Central Japan, analyzed by the minor structures in its southwestern area: *Japan J. Geol. Geog.*, v. 37, p. 63-85.
- Kulm, L. D., von Huene, R., et al., 1973. Initial Reports of the Deep Sea Drilling Project, Volume 18: Washington (U.S. Government Printing Office).
- Matsuda, T., 1962. Crustal deformation and igneous activity in the south Fossa Magna, Japan: *In Macdonald, G. A. and Kano, H. (Eds.), Am. Geophys. Union, Geophys. Mono 6*, p. 140-150.
- Moore, J. C., 1973. Complex deformation of Cretaceous trench deposits; southwestern Alaska: *Geol. Soc. Am. Bull.*, v. 84, p. 2005-2020.
- Silver, E. A., 1972. Pleistocene tectonic accretion of the continental slope off Washington: *Marine Geol.*, v. 13, p. 239-249.
- von Huene, R., 1972. Structure of the continental margins and tectonism of the eastern Aleutian Trench: *Geol. Soc. Am. Bull.*, v. 83, p. 3613-3626.

APPENDIX A
Summary of X-Ray, Grain Size, and Carbon-Carbonate Results, Site 298

Section	Sample Depth Below Sea Floor (m)	Lithology	Age	Bulk Sample Major Constituent			2-20 μ m Fraction Major Constituent			<2 μ m Fraction Major Constituent			Grain Size			Classification	Carbon Carbonate			Comments
				1	2	3	1	2	3	1	2	3	Sand (%)	Silt (%)	Clay (%)		Total (%)	Organic (%)	CaCO ₂ (%)	
				298A-1-1	51.9	Unit 1 Silty Clay, Clayey and Silty Sand	Late Pleistocene to Holocene(?)	Quar.	Plag.	Mica	Quar.	Plag.	Mica	Mica	Quar.		Plag.	2.1	53.3	
298-2-3	130.7	Quar.	Mica	Plag.	Quar.			Plag.	Mica	Mica	Quar.	Mont.	8.9	52.9	38.1	Clayey Silt	0.5	0.4	1	
298-5 2	195.8	Unit 2 Claystone, Silty Claystone Clay, Silty Clay and Clayey, and Silty Sands	Early Pleistocene	Quar.	Plag.	Mica	Quar.	Plag.	Mica	Mica	Quar.	Mont.	5.0	72.6	22.4	Clayey Silt	0.9	0.4	3	Amph. in bulk (1.1%), 2-20 μ m (1.1%)
298-6-2	280.9-281.0			Quar.	Plag.	Mica	Quar.	Plag.	Mica	Mica	Quar.	Plag.	3.7	59.8	36.5	Clayey Silt	0.8	0.5	2	
298-7-1	298.2			Quar.	Plag.	Mica	Quar.	Plag.	Mica	Mica	Quar.	Plag.	0.2	50.4	49.4	Clayey Silt				
298-8-1	317.8			Quar.	Plag.	Mica	Quar.	Plag.	Mica	Mica	Quar.	Plag.	0.4	53.4	46.3	Clayey Silt				
298-9-1	336.8			Quar.	Mica	Plag.	Quar.	Plag.	Mica	Mica	Quar.	Plag.	0.1	46.6	53.3	Silty Clay	1.2	0.6	5	
298-10 4	368.9			Quar.	Mica	Plag.	Quar.	Plag.	Mica	Mica	Quar.	Plag.	0.0	39.8	60.2	Silty Clay	0.9	0.6	3	
298-11-2	394.1			Quar.	Mica	Plag.	Quar.	Plag.	Mica	Mica	Quar.	Plag.	0.0	53.1	46.9	Clayey Silt	0.9	0.5	3	
298-11-3	395.6			Quar.	Mica	Plag.	Quar.	Plag.	Mica	Mica	Quar.	Plag.	0.0	53.9	46.1	Clayey Silt	0.8	0.5	3	
298-14-2	518.6			Quar.	Mica	Plag.	Quar.	Plag.	Mica	Mica	Quar.	Plag.	0.2	54.6	45.2	Clayey Silt	0.8	0.5	3	
298-15 5	570.3			Quar.	Mica	Plag.	Quar.	Plag.	Mica	Mica	Quar.	Plag.	0.2	54.6	45.2	Clayey Silt	0.8	0.5	3	
298-16 2	604.3	Quar.	Mica	Plag.	Quar.	Plag.	Mica	Mica	Quar.	Mont.	0.0	52.0	48.0	Clayey Silt	0.8	0.5	3			

Note: Complete results X-ray, Site 298, will be found in Part V, Appendix I. X-ray mineralogical legend on Appendix A, Chapter 2.

Site 298 Hole Core 1 Cored Interval: 0.0-3.0 m

AGE	ZONE	FOSSIL CHARACTER					METERS	LITHOLOGY	DEFORMATION	LITHO. SAMPLE	LITHOLOGIC DESCRIPTION
		FORAMS	NAANOS	RADS	SILICO. DIATOMS	SECTION					
PLEISTOCENE-HOLOCENE	Emiliana huxleyi Pseudonotia dolioleus (D)	BF	Ag	Fm	Rm	Rm	0.5	VOID			Unit 1. Drilling deformation - soupy; color dark green gray (5GY 4/1); core is basically silty sand with lithified rock fragments. SILTY SAND Smear: CC Texture 50% Sand 40% Silt 10% Clay Composition 30% Quartz 25% Lithic fragments 18% Heavy minerals 10% Clay minerals 5% Volcanic glass 5% Foraminifera 5% Feldspar 5% Mica 2% Sponge spicules Lithified fragments in silty sand matrix. 1) CALCAREOUS SILT-RICH SANDSTONE (Binocular description) Texture 70% Sand 15% Silt 15% Clay Composition 45% Quartz 25% Feldspar 15% Authigenic carbonate 8% Mica 5% Clay minerals 2% Heavy minerals Tr% Foraminifera 2) LIMESTONE Smear: CC Texture 85% Silt 10% Sand 5% Clay Composition 75% Carbonate (unspecified) 10% Clay minerals 10% Feldspar 1% Mica 3) SILTY CLAYSTONE
							1.0		OOO	CC	
							Core Catcher				

Explanatory notes in chapter 1

Site 298 Hole Core 2 Cored Interval: 126.5-130.0 m

AGE	ZONE	FOSSIL CHARACTER					METERS	LITHOLOGY	DEFORMATION	LITHO. SAMPLE	LITHOLOGIC DESCRIPTION
		FORAMS	NAANOS	RADS	SILICO. DIATOMS	SECTION					
PLEISTOCENE-HOLOCENE	Emiliana huxleyi Pseudonotia dolioleus (D)	BF	Cg	Cm	Fg	B	0.5	VOID			Colors: Sand - olive black (5Y 2/1); clayey silts - dark green gray (5GY 4/1); interbedded units, some grading and some rounded silty claystone fragments noted: 1-99, 1-116, 2-110 to 130, 3-105, 4-150 and CC; intense-moderate drilling deformation; clam borings in silty claystone (Section 4); claystone has a weathering rind. 5Y 5/2 CLAYEY SILT Smear: CC Texture 50% Silt 45% Clay 5% Sand Composition 44% Clay minerals 20% Quartz 10% Feldspar 8% Nannofossils 5% Volcanic glass 3% Plant Debris 3% Diatoms 2% Heavy minerals 1% CO ₂ unspecified 1% Foraminifera, radiolarians Tr% Glauc., sponge spicules LITHIFIED FRAGMENT SILTY CLAYSTONE (Minor Lith) Smear: CC Texture 85% Clay 15% Silt Composition 85% Clay minerals 7% Quartz 5% Volcanic glass 2% Feldspar 1% Heavy minerals Tr% Lithic fragments Tr% Nannofossils Tr% Sponge spicules CLAYEY SAND Smear: 2-15 Texture 70% Sand 30% Clay 10% Silt Composition 27% Quartz (2% poly-quartz) 25% Clay minerals 20% Lithic fragments 15% Feldspar 3% Heavy minerals 3% Plant debris 1% Mica 1% Glauconite 1% Nannofossils 1% Diatoms Grain Size 3-118 8.9, 52.9, 38.1 Carbon Carbonate 3-121 0.5, 0.4, 1 X-ray 3-120 (Bulk) 39.5% Quar 25.4% Mica 24.9% Plag 5.4% Chlo 3.7% Mont 1.1% Amph
							1.0				
							Core Catcher				

Explanatory notes in chapter 1

Site 298 Hole Core 3 Cored Interval: 174.0-183.5 m

AGE	ZONE	FOSSIL CHARACTER				METERS	LITHOLOGY	DEFORMATION	LITHO. SAMPLE	LITHOLOGIC DESCRIPTION
		FORAMS	NANNOSS	RADS	SILICO. DIATOMS					
PLEISTOCENE-HOLOCENE	Emiliania huxleyi Pseudoeunotia dolliolus (D)	Fg	Rm			0.5	VOID			Colors grayish black (N2) to dark gray (N3); semi-consolidated - slight drilling deformation. SAND/SILT-RICH CLAY Smear: CC Texture 65% Clay 20% Silt 15% Sand Composition 55% Clay minerals 20% Quartz, feldspar 7% Volcanic glass 5% Heavy minerals 2% Radiolarians 1% Nannofossils 1% Sponge spicules Tr% Glauconite Tr% Foraminifera
		B	Cm	Fm		1.0	Core Catcher			
										N2/N3 * CC

Explanatory notes in chapter 1

Site 298 Hole Core 4 Cored Interval: 183.5-193.0 m

AGE	ZONE	FOSSIL CHARACTER				METERS	LITHOLOGY	DEFORMATION	LITHO. SAMPLE	LITHOLOGIC DESCRIPTION
		FORAMS	NANNOSS	RADS	SILICO. DIATOMS					
LATE PLEISTOCENE	Emiliania huxleyi Gephyrocapsa oceanica Pseudoeunotia dolliolus (D)	B				0.5	VOID			Basic color, dark gray (N3) with areas of greenish gray (5G7 6/1); alternations of fissile clayey silt - clayey siltstone with indurated-semi-indurated zones (not fragments); some burrows and laminations noted; distinct bedding boundaries occur with sandy zones SILTY CLAY Smears: 3-80, CC Texture 50% Silt 45% Clay 5% Sand Composition 32-40% Clay minerals 20-25% Quartz 15% Nannofossils 10% Lithic fragments 5% Feldspar 5% Volcanic glass 3-10% Heavy minerals 3% Radiolarians 1% Mica Tr% Zeolite Tr% Foraminifera Tr% Glauconite
		Cm				1.0	VOID			
		Rg	Fm	Rm		2	VOID			N3 * 20 * 80 * 147 * CC
										SILT-RICH SAND (Minor Lith) Smear: 3-147 Texture 75% Sand 20% Silt 5% Clay Composition 68% Lithic fragments 10% Clay minerals 10% Quartz 5% Heavy minerals 2% Volcanic glass 2% Glauconite 2% Micarb 1% Feldspar Tr% Foraminifera Tr% Sponge spicules
										LITHIFIED PEBBLE FRAGMENT CLAYEY LIMESTONE (Minor Lith) Smear: 1-20 Texture 100% Clay Composition 75% Authigenic carbonate 25% Clay minerals Tr% Quartz

Explanatory notes in chapter 1

Site 298 Hole Core 5 Cored Interval: 193.0-202.5 m

AGE	ZONE	FOSSIL CHARACTER				METERS	LITHOLOGY	DEFORMATION	LITHO. SAMPLE	LITHOLOGIC DESCRIPTION
		FORAMS	NANNOSS	RADS	SILICO. DIATOMS					
LATE PLEISTOCENE	Gephyrocapsa oceanica Pseudoeunotia dolliolus (D)	Fm	B	B		0.5	VOID			Color dominantly dark gray (N3); moderate to intense drilling deformation; clayey limestone fragment (Section 1, 120 cm.) Base of fragment defines Unit 1-2 boundary. SILT-RICH CLAYEY SAND Smear: 2-93 Texture 45% Sand 35% Clay 20% Silt Composition 35% Clay minerals 35% Quartz 20% Lithic fragments 5% Feldspar 1% Mica 1% Volcanic glass 1% Glauconite 1% Zeolite Tr% Micarb Tr% Sponge spicules
		Cm				1.0	VOID			
						2	VOID			N3 N4 N3 N4 N3 * 90 * 93 * CC *
										VOLCANIC ASH (Minor Lith) Smear: 2-90 Texture 75% Sand 20% Silt 5% Clay Composition 86% Volcanic glass 7% Quartz 3% Lithic fragments 2% Clay minerals 1% Heavy minerals 1% Glauconite 1% Micarb 1% Nannofossils
										CLAYEY SILT Smear: CC Texture 50% Silt 45% Clay 5% Sand Composition 60% Clay minerals 30% Quartz, feldspar 5% Nannofossils 2% Mica 1% Volcanic glass 1% Micarb Tr% Glauconite Tr% Foraminifera
										Grain Size 2-131 (from lower portion, but not 5.0, 72.6, 22.4 base of graded bed) Carbon Carbonate 2-135 0.9, 0.4, 3 X-ray 2-133 (Bulk) 46.8% Quar 28.3% Plag 16.2% Mica 5.6% Calc 3.0% Chlo

Explanatory notes in chapter 1

Site 298 Hole Core 6 Cored Interval: 278.5-288.0 m

AGE	ZONE	FOSSIL CHARACTER				METERS	LITHOLOGY	DEFORMATION	LITHO. SAMPLE	LITHOLOGIC DESCRIPTION
		FORAMS	NANNOS	RADS	SILICO DIATOMS					
LATE PLEISTOCENE	Gephyrocapsa oceanica Pseudoemotia doitloius (D)	Fm				0.5			96 *	Color - olive black (5Y 2/1); drilling deformation slight(?); hackly fracture with fabric < 1 mm thick; no bedding visible; inclination of fissile fabric (possibly bedding) may define small scale folds or could represent conjugate fractures due to drilling.
		B				1.0				
LATE PLEISTOCENE	Gephyrocapsa oceanica Pseudoemotia doitloius (D)	B				2.0			CC *	CLAYEY SILT Smears: 1-96, CC Texture 55% Silt 41% Clay 4% Sand Composition 59-65% Clay minerals 15-20% Quartz 7-10% Heavy minerals 3% Nannofossils 3- 5% Feldspar 1% Diatoms Tr- 3% Volcanic glass Tr- 2% Zeolite Tr- 2% Lithic fragments Tr- 2% Radiolarians Tr- 1% Sponge spicules Tr- 1% Glauconite
		Rp				2.0				
						Core Catcher				Grain Size 2-90 3.7, 59.8, 36.5 X-ray 2-95 (Bulk) 40.7% Quar 28.3% Plag 22.7% Mica 4.2% Chlo 4.2% Mont Carbon Carbonate 2-90 0.8, 0.5, 2

Explanatory notes in chapter 1

Site 298 Hole Core 7 Cored Interval: 297.5-307.0 m

AGE	ZONE	FOSSIL CHARACTER				METERS	LITHOLOGY	DEFORMATION	LITHO. SAMPLE	LITHOLOGIC DESCRIPTION
		FORAMS	NANNOS	RADS	SILICO DIATOMS					
LATE PLEISTOCENE	Gephyrocapsa oceanica	Fg				0.5			67 *	Color olive black (5Y 2/1); strong fissility locally cross-cut by hackly fractures; minor silt beds - grey black (N2); horizontal shale bedding parallel to fissility; slight to minor drilling deformation
		B				1.0				
LATE PLEISTOCENE	Gephyrocapsa caribbeanica Subzone Pseudoemotia doitloius (D)	B				2.0			N2	CLAYEY SILTSTONE (Shale) Smear: 1-67 Texture 51% Silt 49% Clay Composition 86% Clay minerals 8% Feldspar 3% Volcanic glass 2% Quartz 1% Heavy minerals Tr% Micarb Tr% Diatoms Tr% Radiolarians Tr% Sponge spicules
		Rp				2.0				
EARLY PLEISTOCENE	Gephyrocapsa caribbeanica Subzone Pseudoemotia doitloius (D)	B				2.0			N2	CLAYEY SILTSTONE (Shale) Smear: 1-67 Texture 51% Silt 49% Clay Composition 86% Clay minerals 8% Feldspar 3% Volcanic glass 2% Quartz 1% Heavy minerals Tr% Micarb Tr% Diatoms Tr% Radiolarians Tr% Sponge spicules
		Cg				2.0				
						Core Catcher				Grain Size 1-67 0.2, 50.4, 49.4

Explanatory notes in chapter 1

Site 298 Hole Core 8 Cored Interval: 316.5-326.0 m

AGE	ZONE	FOSSIL CHARACTER				METERS	LITHOLOGY	DEFORMATION	LITHO. SAMPLE	LITHOLOGIC DESCRIPTION
		FORAMS	NANNOS	RADS	SILICO DIATOMS					
EARLY PLEISTOCENE	Gephyrocapsa caribbeanica Subzone Pseudoemotia doitloius (D)	B				0.5	VOID		135 *	Color olive gray (5Y 2/1); very fissile with slight drilling deformation. Structural observations: 2-65 to 75 cm, hackly fractures (possible cleavage) inclined 25° to bedding (dipping 5°); 2-135 to 145 cm, well defined fractures inclined at 65°, probable drilling induced fractures.
		Fg				1.0				
EARLY PLEISTOCENE	Gephyrocapsa caribbeanica Subzone Pseudoemotia doitloius (D)	B				2.0			5Y 2/1	CLAYEY SILTSTONE (Shale) Smear: 1-135 Texture 54% Silt 46% Clay Composition 68% Clay minerals 20% Quartz 15% Feldspar 5% Mica 5% Sponge spicules 4% Nannofossils 2% Volcanic glass 1% Diatoms Tr% Radiolarians
		Rp				2.0				
						Core Catcher				Grain Size 1-133 0.4, 53.4, 46.3

Explanatory notes in chapter 1

Site 298		Hole		Core 11		Cored Interval: 392.5-402.0 m						
AGE	ZONE	FOSSIL CHARACTER				SECTION	METERS	LITHOLOGY	DEFORMATION	LITHO. SAMPLE	LITHOLOGIC DESCRIPTION	
		FORAMS	NANNOIDS	RADS SILICO.	DIATOMS							
EARLY PLEISTOCENE	<i>Gephyrocapsa caribbeanica</i> Subzone					1	0.5	VOID			<p>Colors - medium dark gray (N4) to dark green gray (5GY 4/1); slight drilling deformation; bedding planes irregular to horizontal, poor to moderate fissility; some variegated laminae, weakly developed and thick to thin; bedding inclinations: Section 1, 14°; Section 2, 7-10°; Section 3, 6-10°; and Section 4, 0-5°; at Section 4 (125 cm) silt beds show scour marks and load casts indicating upright beds.</p> <p>CLAYEY SILTSTONE (Shale)</p> <p>Grain Size 3-14 0.0, 53.1, 46.9</p> <p>Carbon Carbonate 2-13 0.9, 0.6, 3</p> <p>X-ray 3-14 (Bulk) 38.0% Quar 27.0% Mica 25.6% Plag 6.3% Chlo 3.1% Mont</p>	
						2	1.0					
						3		CONSOLIDATION SAMPLE				5GY 4/1-N4
						4		GEOCHEM SAMPLE				
				B	Cg	B	B			VOID		
						Core Catcher						

Explanatory notes in chapter 1

Site 298		Hole		Core 12		Cored Interval: 421.0-430.5 m																																																											
AGE	ZONE	FOSSIL CHARACTER				SECTION	METERS	LITHOLOGY	DEFORMATION	LITHO. SAMPLE	LITHOLOGIC DESCRIPTION																																																						
		FORAMS	NANNOIDS	RADS SILICO.	DIATOMS																																																												
EARLY PLEISTOCENE	<i>Gephyrocapsa caribbeanica</i> Subzone <i>Pseudonotella dolliolus</i> (D)					1	0.5	VOID			<p>Medium dark gray (N4) to dark greenish gray (5GY 4/1); slight drilling deformation, faint fissility; horizontal bedding with some color bands; some inclined bedding (Section 4); broken chunky portions (50-70 cm) in Section 4; bedding inclined 0-10°; hackly fractures (cleavage?) dip 12-30°; Section 5 (60-76 cm), graded bed becomes finer up-core indicating upright beds.</p> <p>SILTY CLAYSTONE (Shale)</p> <p>Smear: CC</p> <table border="0"> <tr> <td>Texture</td> <td>Composition</td> </tr> <tr> <td>55% Clay</td> <td>65% Clay minerals</td> </tr> <tr> <td>40% Silt</td> <td>15% Quartz</td> </tr> <tr> <td>5% Sand</td> <td>5% Feldspar</td> </tr> <tr> <td></td> <td>3% Mica</td> </tr> <tr> <td></td> <td>3% Volcanic glass</td> </tr> <tr> <td></td> <td>3% Nannofossils</td> </tr> <tr> <td></td> <td>2% Heavy minerals</td> </tr> <tr> <td></td> <td>2% Zeolite</td> </tr> <tr> <td></td> <td>1% Sponge spicules</td> </tr> <tr> <td></td> <td>1% Radiolarians</td> </tr> <tr> <td></td> <td>Tr% Pyrite</td> </tr> <tr> <td></td> <td>Tr% Diatoms</td> </tr> <tr> <td></td> <td>Tr% Glauconite</td> </tr> </table> <p>5GY 4/1 + N4</p> <p>SILTY SAND (Minor Lith)</p> <p>Smear: 5-50</p> <table border="0"> <tr> <td>Texture</td> <td>Composition</td> </tr> <tr> <td>65% Sand</td> <td>35% Quartz</td> </tr> <tr> <td>25% Silt</td> <td>25% Lithic fragments</td> </tr> <tr> <td>10% Clay</td> <td>18% Clay minerals</td> </tr> <tr> <td></td> <td>15% Heavy minerals</td> </tr> <tr> <td></td> <td>10% Volcanic glass</td> </tr> <tr> <td></td> <td>5% Feldspar</td> </tr> <tr> <td></td> <td>1% Carbonate fragments</td> </tr> <tr> <td></td> <td>1% Sponge spicules</td> </tr> <tr> <td></td> <td>Tr% Foraminifera</td> </tr> <tr> <td></td> <td>Tr% Glauconite</td> </tr> <tr> <td></td> <td>Tr% Radiolarians</td> </tr> <tr> <td></td> <td>Tr% Diatoms</td> </tr> </table>	Texture	Composition	55% Clay	65% Clay minerals	40% Silt	15% Quartz	5% Sand	5% Feldspar		3% Mica		3% Volcanic glass		3% Nannofossils		2% Heavy minerals		2% Zeolite		1% Sponge spicules		1% Radiolarians		Tr% Pyrite		Tr% Diatoms		Tr% Glauconite	Texture	Composition	65% Sand	35% Quartz	25% Silt	25% Lithic fragments	10% Clay	18% Clay minerals		15% Heavy minerals		10% Volcanic glass		5% Feldspar		1% Carbonate fragments		1% Sponge spicules		Tr% Foraminifera		Tr% Glauconite		Tr% Radiolarians		Tr% Diatoms
		Texture	Composition																																																														
		55% Clay	65% Clay minerals																																																														
		40% Silt	15% Quartz																																																														
		5% Sand	5% Feldspar																																																														
	3% Mica																																																																
	3% Volcanic glass																																																																
	3% Nannofossils																																																																
	2% Heavy minerals																																																																
	2% Zeolite																																																																
	1% Sponge spicules																																																																
	1% Radiolarians																																																																
	Tr% Pyrite																																																																
	Tr% Diatoms																																																																
	Tr% Glauconite																																																																
Texture	Composition																																																																
65% Sand	35% Quartz																																																																
25% Silt	25% Lithic fragments																																																																
10% Clay	18% Clay minerals																																																																
	15% Heavy minerals																																																																
	10% Volcanic glass																																																																
	5% Feldspar																																																																
	1% Carbonate fragments																																																																
	1% Sponge spicules																																																																
	Tr% Foraminifera																																																																
	Tr% Glauconite																																																																
	Tr% Radiolarians																																																																
	Tr% Diatoms																																																																
						2	1.0																																																										
						3																																																											
						4																																																											
		Rg	Cg	Rp	Rm			VOID			5GY 4/1																																																						
						Core Catcher					5GY 4/1																																																						

Explanatory notes in chapter 1

Site 298 Hole Core 15 Cored Interval: 563.5-573.0 m

AGE	ZONE	FOSSIL CHARACTER				METERS	LITHOLOGY	DEFORMATION	LITHO. SAMPLE	LITHOLOGIC DESCRIPTION
		FORAMS	NANNOS	RADS	SILICO. DIATOMS					
EARLY PLEISTOCENE	Gephyrocapsa caribbeanica Subzone					0.5			Color olive gray (5Y 3/2); slight drilling deformation, graded beds (overturned) 2-10 cm thick; bedding dip 8°-26°; hackly fractures inclined 9°; Section 1 (0-10) 5 cm thick beds graded silt to burrowed clay toward base of core (section overturned); Section 2 - various beds, 2-10 cm thick beds graded silt-clay towards base of core, (section overturned); Section 3 - various overturned graded beds. CLAYEY SILTSTONE (Shale) Smear: 5-80 Texture 55% Silt 45% Clay Composition 42% Clay minerals 25% Quartz 15% Feldspar 10% Volcanic glass 5% Heavy minerals 3% Nannofossils Locally ash-rich. Grain Size 5-80 0.2, 54.6, 45.2 Carbon Carbonate 5-80 0.8, 0.5, 3 X-ray 5-80 (Bulk) 38.7% Quar 29.6% Mica 21.1% plag 6.6% Chlo 4.0% Mont	
						1				
						1.0				
		B B				2				
						3				5Y 3/2
						4		GEOCHEM SAMPLE		
				5		5Y 3/1				
				6		56Y 4/1				
		Fg	B	B	B	Core Catcher	5Y 3/2			

Explanatory notes in chapter 1

Site 298 Hole Core 16 Cored Interval: 601.5-611.0 m

AGE	ZONE	FOSSIL CHARACTER				METERS	LITHOLOGY	DEFORMATION	LITHO. SAMPLE	LITHOLOGIC DESCRIPTION
		FORAMS	NANNOS	RADS	SILICO. DIATOMS					
EARLY PLEISTOCENE	Gephyrocapsa caribbeanica Subzone					0.5	VOID			Color dark green gray (5GY 4/1); slight drilling deformation; bedding (12-15°); laminations, thick and thin, variable; hackly fractures - horizontal; graded beds indicate core overturned; Section 1 (96-101 cm), overturned graded bed (silt-clay downward), sole marking or scouring at 96 cm confirm overturning; Section 3 (7-17 cm) graded bed fines downward indicating overturning; Section 5 (132-135 cm) graded bed, fines downward indicating overturning. CLAYEY SILTSTONE (Shale) Smear: 2-130 Texture 52% Silt 48% Clay Composition 35% Clay minerals 25% Quartz 15% Feldspar 10% Heavy minerals 7% Volcanic glass 5% Lithic fragments 2% Nannofossils 1% Micarb Grain Size 2-130 0.0, 52.0, 48.0 Carbon Carbonate 2-130 0.8, 0.5, 3 X-ray 2-130 (Bulk) 39.5% Quar 24.6% Mica 23.1% Plag 5.7% Chlo 5.5% Mont 1.2% Amph
						1				
						1.0				
						2	GEOCHEM AND CONSOLIDATION SAMPLE	13Q		
						3		56Y 4/1		
						4		56Y 4/1		
				5		56Y 4/1				
		B	Cg	B	B	Core Catcher	56Y 4/1			

Explanatory notes in chapter 1

AGE	ZONE	FOSSIL CHARACTER					SECTION METERS	LITHOLOGY	DEFORMATION	LITHO. SAMPLE	LITHOLOGIC DESCRIPTION
		FORAMS	NANNOS	SANDS	COCCO-LITHO	DIATOMS					
LATE PLEISTOCENE-HOLOCENE	N23 Emiliania huxleyi Pseudonostoc dollfus (D)	Cg	Cg	Fg	Bl	dy	0.5 1 1.0	VOID			Unit 1. Color olive black (5Y 4/1); very deformed by drilling mixed sand-silty clay. SAND Smear: * Texture 100% Sand Composition 82% Lithic fragments 15% Feldspar 5% Quartz 3% Heavy minerals Tr% Glauconite CLAYEY SILT Smear: * Texture 53% Silt 47% Clay 2% Sand Composition 45% Clay minerals 30% Quartz 15% Feldspar 2% Opaques 2% Volcanic glass 2% Heavy minerals 1% Sponge spicules 1% Radiolarians 1% Mica 1% Diatoms 1% Nannofossils *Smears from sediment on heat probe container. Grain Size 1-139 Carbon Carbonate 1-138 2.1, 53.3, 44.6 0.6, 0.5, 0 X-ray 1-147 (Bulk) 43.6% Quar 24.7% Plag 22.3% Mica 4.8% Chlo 4.6% Mont
							Core Catcher				

Explanatory notes in chapter 1

